JOURNAL OF Applied Polymer SCIENCE

Application of Melt-Blown Technology for the Manufacture of Temperature-Sensitive Nonwoven Fabrics Composed of Polymer Blends PP/PCL Loaded with Multiwall Carbon Nanotubes

Izabella Krucińska, Beata Surma, Michał Chrzanowski, Ewa Skrzetuska, Michał Puchalski
Centre of Advanced Technologies of Human-Friendly Textiles "Pro Humano tex," Department of Material and Commodity Sciences and Textile Metrology, Faculty of Material Technologies and Textile Design, Technical University of Lodz, 90-924 Lodz, Poland

Correspondence to: I. Krucińska (E-mail: ikrucins@p.lodz.pl)

ABSTRACT: The main aim of this research was to detail the use of melt-blown technology to manufacture a temperature-sensitive nonwoven fabric. The sensor properties of the fabric were achieved by application of the optimal composition of immiscible polymer blends loaded with multiwall carbon nanotubes (MWCNTs). As the sensing phase, a dispersion of MWCNTs in poly(ε-caprolactone) (PCL) was used. The sensing phase was blended with a matrix made of polypropylene (PP). Three different polymer compositions were subjected to the melt-blowing process, changing the proportion of the matrix polymer to the dispersed phase to the range of 50–70% and changing the MWCNTs content to be between 1.2 and 2%. The selection of technological parameters was based on the thermal characteristics of the polymers used. Nonwoven fabrics made of these composites were characterized by measuring their electrical properties as a function of external stimuli. In particular, their responses to cycle changing of temperature in a range of 20–80°C were monitored. The 70%PP/28.8%/1.2%MWCNT nonwoven fabrics were observed to show the best sensitivity to changes in temperature between 50 and 60°C. © 2012 Wiley Periodicals, Inc. J. Appl. Polym. Sci. 000: 000–000, 2012

KEYWORDS: sensors and actuators; nanocomposites; polymer blends; carbon nanotubes

Received 22 July 2011; accepted 29 March 2012; published online
DOI: 10.1002/app.37834

INTRODUCTION

In 1991, Iijima discovered multiwall carbon nanotubes (MWCNTs) while synthesizing fullerenes,[1] and about 2 years later, he observed single-wall carbon nanotubes (SWCNTs).[2] Both are composed of hexagonal carbon lattices formed into tiny tubes characterized by unique properties, which depend on the overall morphology, atomic arrangement, chirality, diameter, and length of the tubes.[3–5] The application of carbon nanotubes (CNTs), which are referred to as the diamond of the 21st century because of their exceptional mechanical, thermal, and electrical properties, has had a strong influence on the development of a new class of composite materials with diverse applications. The first polymer nanocomposites using CNTs were described by Ajayan et al.[6] in 1994. Six years later, the first technologies regarding the manufacture of nanocomposite fibers reinforced with nanotubes were described by Haggenmueller et al.[7] and Vigolo et al.[8]

Haggenmueller et al. used melt mixing to disperse SWCNTs in poly(methyl methacrylate) (PMMA). The reinforcement of PMMA fibers with SWCNTs resulted in the improvement in mechanical properties of the obtained fibers. A maximum modulus of 7 GPa was observed for a draw ratio of 100, and maximum fiber strength of 130 MPa was achieved at a very high draw ratio of 900. Vigolo et al. applied the wet spinning method to form SWCNT fibers with the aid of polyvinyl alcohol (PVA) dissolved in water. The obtained fibers were characterized by a high Young's modulus of 9–15 GPa and a tensile strength of 150 MPa. Wet stretching of the SWCNT fibers resulted in increases in the modulus up to 40 GPa and in the strength up to 230 MPa.[9] In 2003, Dalton et al.[10] demonstrated that leaving PVA polymer in the fibers resulted in increases in the Young's modulus up to 80 GPa and in the strength up to 1.8 GPa. Fibers made from SWCNTs and PVA spun using DNA as the dispersant were investigated by Barisci et al.[11] Fibers fabricated from polypropylene (PP) and SWCNTs were the subject of research by Kearns and Shambaugh in 2002.[12] PP–SWCNT fibers were also spun by Moore et al.,[13] Miaudet et al.,[14] and Chang et al.[15] Gao et al.[16] spun polyamide (PA6)/SWCNT nanocomposite fibers, applying ring-opening polymerization of

caprolactam in the presence of SWCNTs. The improvement in mechanical properties afforded by applying SWCNTs has also been achieved for electrospun fibers. Ko et al.[17] produced polyacrylonitrile (PAN)/SWCNT fibers with an enhanced Young's modulus of 140 GPa, and Sen et al.[18] spun polystyrene and polyurethane fibers reinforced with SWCNTs.

The improvement in the mechanical properties of nanocomposite fibers was the first challenge to be met by researchers. The second was to develop a new class of sensor materials by the incorporation of CNTs into polymeric matrices.

Until now, intensive research has been carried out toward the development of CNTs/polymer sensor films that provide information on the physical,[19,20] chemical,[21–28] and biological properties of a given environment.[29,30] Few studies have been reported regarding CNTs/polymer sensors produced by the application of textile technologies.[31–33] The development of fibrous sensors can play an important role in increasing the sensitivity of materials because of their highly developed porous structure, which results in a high surface area per unit mass of the sensors (specific surface area). One of the first fibrous sensors was reported by Feller and Grohens in 2004.[31] They described the manufacture of monofilaments using poly(amide12-*b*-tetramethylene oxide)–carbon black and poly(ethylene-*co*-ethyl acrylate)–carbon black. Changes in the electrical resistance of the developed monofilaments were observed under the influence of organic solvent vapors, i.e., chloroform and toluene. The idea of developing polymer sensors was based on the incorporation of electroconductive black carbon particles (CB) into polymer matrices. A similar idea was used by Cochrane et al.[32,33] in developing a strain sensor printed on a textile substrate. The favorable results obtained for the intelligent textiles based on polymer/CB materials stimulated research on a new form of fibers composed of CNTs. In 2010, Pötschke et al.[34] generated polylactide (PLA) monofilaments reinforced with MWCNTs that possessed the ability to detect the presence of different solvents, such as water, *n*-hexane, ethanol, and methanol. Krucińska et al.[35] applied electrospinning technology to produce the vapor-sensing nonwoven fabric made of PEO/MWCNTs. In their other article, Krucińska et.al.[36] demonstrated a printing technology that used MWCNTs for the manufacture of fabrics with the ability to detect the mechanical loads.

There are many textile technologies that can be explored for the development of new classes of intelligent textiles. The attention of researchers has mainly been drawn to wet and melt spinning or printing. One textile technique that is potentially useful for the development of a new class of sensors is melt-blown technology. Beginning with a polymer mixture, melt-blown technology allows one to obtain a final product in the form of a nonwoven material manufactured through a highly cost-effective one-step process. Therefore, the main aim of this article is to demonstrate the applicability of melt-blown technology to the manufacture of temperature-sensitive textile products.

The polymer most commonly used in melt-blown technology is PP. To achieve the desired sensing properties in the investigated materials, we explored the use of conductive immiscible polymer blends described by Srivastava et al.[37] In selected immiscible blends, PP serves as the semicrystalline matrix, and poly (ε-caprolactone) (PCL) serves as the dispersant for CNTs. We assume that enhancement in the conductivity of these blends results from the attraction of CNTs by PCL and from the localization of carbon particles at the PP/PCL interface. It was assumed that the mechanism of temperature-sensing results from positive temperature coefficient (PTC) effects[38] at increased temperatures near 60°C, where a phase change in PCL and a conductor-to-insulator transition can be observed. The experiments were designed to investigate the influence of the composition of the polymeric matrix PP/PCL/CNTs on the temperature-sensing properties of melt-blown nonwoven fabrics.

MATERIALS AND EXPERIMENTAL METHODS

Raw Materials

For the manufacture of nonwoven fabrics, a mixture of PP and PCL with MWCNTs was prepared through a two-stage process. In the first stage, PCL CAPA6400 with a molar mass of 37,000 delivered by Perstrop UK was used. The selected grade of PCL is characterized by a high melt flow ratio equal to 40 g/10 min determined at 160°C according to ISO 1133. CAPA6400 was melt mixed with MWCNTs Nanocyl®7000 delivered by Nanocyl S.A. Belgium. Nanotubes of 90% purity with diameters of 9.5 nm and lengths of 1.5 μm were produced via catalytic carbon vapor deposition. In the second stage, the nanocomposite polymer PCL/MWNTs was melt mixed with PP HP462R delivered by Basell Polyolefins Moplen and characterized by a melt flow ratio equal of 25 g/10 min (at 260°C and 2.16 kg) determined according to standard ISO 1133.

Thermal Behavior of Compound Polymers

To adjust the proper range of temperatures applied during the manufacturing of polymer master batches and melt-blown nonwoven fabrics, thermal analysis was completed using melt flow rate (MFR), thermogravimetric analysis (TGA), and differential scanning calorimetry (DSC) methods.

MFR measurements of PCL/4%MWCNTs and the various blends of PP/PCL/4%MWCNTs were done using a Hanatek Melt Flow Indexer UK according to ISO 1133 standard (temperature range 180–300°C/2.16 kg).

The TGA method, which is based on the change in the rate of polymer mass loss during heating, is one of the most significant in studying the thermal properties of polymers. The changes in the weights of polymer compositions as a function of temperature during heating were obtained using a Perkin Elmer TGA 7, Massachusetts US. The specimens were tested using a corundum crucible under a nitrogen flow rate of 25 mL/min in a temperature range from 20 to 600°C.

The thermal analyses of PCL/4%MWCNTs and blends were done using a DSC at a heating rate of 10°C/min (Q 2000 TA Instrument, New Castel US). Two heating cycles were used for each composition. The blends were first heated from 25 to 280°C and then cooled to −30°C and immediately reheated to 280°C.

The mean values of all investigated parameters were determined with a random error equal to 5%.

Melt-Blown Nonwoven Fabrics Preparation

The master batch production was performed in a two-stage process. The first step was performed using a Mini Lab Haake microcompounder twin-screw mixer. PCL pellets dried at a temperature of 50°C for over 24 h and powdery MWCNTs were placed simultaneously into the hopper for gravimetric dosing and were then melt mixed. The temperature applied during the mixing process was ~ 200°C, and the rotation speed of the screws was adjusted to 200 rpm. In the first step, only one PCL/MWCNTs composite was prepared with the weight content of MWCNTs equal to 4%. The second stage was completed using a Mini Lab extruder, and the three following types of composites ware prepared: 50%(PCL/MWCNTs)/50%PP, 40%(PCL/MWCNTs)/60%PP, and 30%(PCL/MWCNTs)/70%PP. The compounding process of master batch production was performed at 200–300°C, adjusting the rotary speed of the screws to 100–360 rpm.

The nonwoven fabrics were produced in the laboratory device schematically shown in Figure 1.

Polymer granules were fed into the hopper, after which they are moved directly into a heated extruder. The extruder has seven adjustable heating zones, which allow for the adequate plasticization of the polymer. The first zone of the extruder is cooled with water to avoid the transition screw temperature in the power transmission system. When the molten polymer is extruded from the die holes, high-velocity hot and dry air streams blow over the droplets of polymer into elementary fibers.

The formed fiber network is located on the collector equipped with an air suction device. The finished product is sent from the drum to the winding frame. The following machine parameters can be adjusted: air temperature, polymer/die temperature, die-to-collector distance, collector speed, polymer throughput, and air throughput. All of these parameters affect the final properties of nonwoven networks.

Experimental Methods for Nonwoven Fabric Characterization

Morphological Properties. The masses and thicknesses of the nonwoven fabrics were determined in accordance with EN29073-1 and EN29073-2 standards, respectively. The mean values of all investigated parameters were determined with a random error equal to 5%.

Crystalline Structure. The supermolecular structures of the fibers forming the nonwoven fabrics were analyzed by wide-angle X-ray scattering. These investigations were undertaken using an X'Pert Pro diffractometer (PANanalytical, Netherlands) with Cu Kα radiation. The accelerating voltage was 40 kV, and the plate current intensity was 30 mA. X-ray scattering patterns were obtained over diffraction angles ranging from 5° to 60° using an X'Celerator semiconducting stripe detector. Deconvolution of the X-ray peaks was performed according to the method proposed by Hindeleh and Jonson and improved and programmed by Rabiej and Rabiej.[39] The degree of crystallinity was calculated as the ratio of the integrated intensity scattered in the crystalline regions to that scattered by the whole sample (over the total domain from both the crystalline and the amorphous regions).

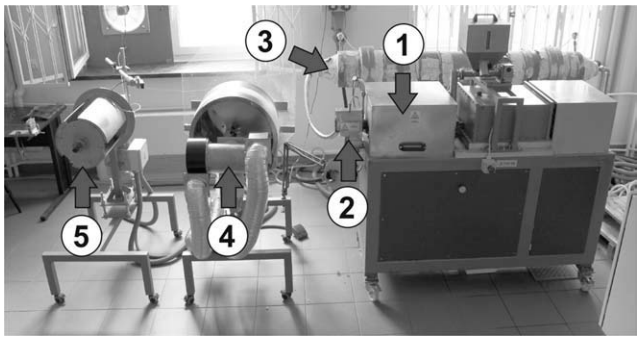

Figure 1. Schematic of laboratory stand for nonwoven production: (1) twin-screw extruder EH16D, (2) die, (3) air-heating system, (4) collector, and (5) winding frame.

Scanning Electron Microscopy. The dimensions of the fibers formed from the PP/PCL/MWCNTs were determined from scanning electron microscope (SEM) micrographs. SEM observations were made using an FEI Nova NanoSEM 230 Netherlands system (low vacuum—0.3 Torr, secondary electron detection). The samples of nonwoven fabric were mounted with carbon adhesive tape. The mean values of fiber dimensions were determined with a random error on the level of 5%.

Electrical Properties. The electrical resistances of the PP/PCL/MWCNTs networks were measured according to EN 1149-1 : 2008 Protective clothing-Electrostatic properties Part 1: Surface resistivity (Test method and requirements) and EN 1149-2 : 1999 Protective clothing-Electrostatic properties Part 2: Test method for measurement of the electrical resistance through a material (vertical resistance). Before the measurements, the nonwoven networks were conditioned by maintaining them under the measuring conditions for 24 h. Conditioning and measurements were performed under isothermal conditions ($t = 23$°C) at a relative humidity value of 25% in the conditioning chamber. The electrical resistances of the networks were measured along the longitudinal directions (to determine the surface resistance) and through the materials (to determine the vertical resistance) in a screened standard measuring system using ring and cylindrical electrodes. A Keithley 610C electrometer and a Statron stabilized power supply of unit type 4218 were used. The mean values of electrical resistance were determined for all types of measurements with a random error equal to 5%.

Sensorial Properties. After basic electrical characterization, the temperature sensitivities of the nonwoven fabrics were investigated. Heating cycles were applied to samples using a source of radiation. One cycle consisted of heating from 25 to 80°C and cooling from 80 to 25°C. The heating and cooling rates were determined based on the melt temperature of PCL (about 60°C). The sample temperature was measured using an Optris Laser SIGHT pyrometer. The changes in electrical resistance were determined with a Keithley multimeter. Collection and processing of the data were carried out with a specially developed program. For each sample, four heating–cooling cycles were conducted, and the temperature and resistance were

Table I. The Viscosity Properties of Polymers Used and Polymer Blends

Type of polymer batch	MFR[a] (g/10 min) 180°C	MFR[a] (g/10 min) 230°C	MFR[a] (g/10 min) 260°C	MFR[a] (g/10 min) 300°C
PCL CAPA 6400	MFR160°C = 40 g/10 min			
PCL/4%MWCNTs pellets	0.45	2.62	5.58	12.83
PP HP462R	8.22	22.99	-	-
50%PP/48%PCL/2%MWCNTs	6.30	17.81	26.40	-
60%PP/38.4%PCL/1.6%MWCNTs	7.96	21.50	33.04	-
70%PP/28.8PCL/1.2%MWCNTs	4.46	31.53	47.70	-

[a]MFR precision: ±0.01 g/10 min.

recorded. Based on the collected data, diagrams of the changes in temperature and resistance as functions of time were generated. The sensitivity of each sample to heat flux was determined by relative changes in resistance, which were calculated separately for each cycle according to formula (1).

$$R_{rel} = \frac{R - R_0}{R_0}, \quad (1)$$

where R_0 is the initial resistance and R is the final resistance. The mean values of R_{rel} for each investigated variant were determined with a random error on the level of 10%.

RESULTS AND DISCUSSION

Rheology and Thermal Analyses

To select the appropriate technological parameters for melt-blow processing, the assessment of MFR was performed in a temperature range from 180 to 300°C.

The rheological behaviors of the PP/PCL/MWCNTs blends are shown in Table I.

The blending process used made the polymer composition more fluid and increased the MFR, probably improving the dispersion of the CNTs. In general, the MFR of the PP/(PCL/4%MWCNTs) blends increased with the decrease in the PCL/4%MWCNTs content in PP.

Table II shows the measured thermal properties and crystallinity degree of pure PP, PCL/4%MWCNTs, and their blends. Table III illustrates the results of DSC analysis of the PP/PCL/MWCNTs blends. The results of TGA and DSC are presented in Figure 2.

The incorporation of nanotubes into the PCL resulted in a slight increase in crystallinity degree and an increase of about 20°C in thermal resistance. The presence of PP in the composite caused a decrease in the thermal properties of the blends.

For the PCL sample, the melting temperature was 59.61°C, and the thermogram shows one endothermic peak of melting with an enthalpy value of 57.10 J/g. Polymer cooling leads to recrystallization at a temperature of 27.14°C with an enthalpy value of 44.60 J/g. Reheating causes melting at a lower temperature of 55.79°C and an enthalpy value of 44.60 J/g, which may result from a lower degree of polymer crystallinity or less perfect crystalline structure. The introduction of 4% nanotubes caused an increase in melting temperature of about 6°C and an enthalpy value of 64.53 J/g. During cooling, recrystallization occurs at 41.32°C, and after the second heating, the enthalpy value and melting temperature are reduced. The melting of PP occurs at 162.88°C with an enthalpy value of 57.03 J/g. Cooling leads to recrystallization at a temperature of 112.53°C and an enthalpy value of 66.61 J/g. During the second heating, the melting temperature is reduced to a value of 159.84°C.

For the composites, the intensity of the melting PP peak decreases. Upon cooling, the melting peak of PCL adopts a lower intensity, and during the second heating, the melting temperature of the sample is slightly reduced. These types of changes in the thermal properties of the blends are related to

Table II. Thermal Properties and Crystallinity Degree of Polymers Used

Polymer	Crystallinity degree of polymer by WAXS method (%)	Temperature (°C)[a] Weight loss 5%	Temperature (°C)[a] Weight loss 50%
PP	42.9	381.42	439.11
PCL CAPA 6400	46.4	405.30	443.30
PCL 4%MWCNT	50.6	425.31	462.10
50%PP/48%PCL/2%MWCNTs	45.5	412.40	472.41
60%PP/38.4%PCL/1.6%MWCNTs	47.8	403.10	479.00
70%PP/28.8PCL/1.2%MWCNTs	51.1	382.51	469.01

[a]Temperature precision: ±0.01°C.

Table III. Results of DSC Analysis Conducted Using Polymer Batches

Sample	Thermogram description	PCL peak		PP peak	
		Heat of fusion (J/g)[a]	Temperature (°C)[b]	Heat of fusion (J/g)[a]	Temperature (°C)[b]
PCL CAPA 6400	First heating	57.10	59.61	–	–
	Cooling	44.60	27.14	–	–
	Second heating	44.60	55,79	–	–
PCL 4%CNT	First heating	64.53	65.99	–	–
	Cooling	58.10	41.32	–	–
	Second heating	61.47	60.99	–	–
PP HP462R	First heating	–	–	57.03	162.88
	Cooling	–	–	66.61	112.53
	Second heating	–	–	61.01	159.84
50%PP/48%PCL/2%CNTs	First heating	23.66	60.98	35.50	160.65
	Cooling	18.74	46.34	39.32	123.90
	Second heating	19.14	57.28	36.11	161.99
60%PP/38.4%PCL/1.6%CNTs	First heating	20.79	61.11	32.07	161.36
	Cooling	15.74	45.68	43.64	124.12
	Second heating	16.30	57.12	40.39	162.16
70%PP/28.8%PCL/1.2%CNTs	First heating	24.22	59.38	58.20	164.43
	Cooling	14.48	48.17	66.52	124.51
	Second heating	18.65	57.13	60.38	162.24

[a]Heat of fusion: ±0.01 J/g, [b]Temperature precision: ±0.01°C.

the compositions and the characteristics of the constituent polymers.

Processing of the CPC Nonwoven Fabrics

The technological parameters of manufacturing conductive polymer composites (CPC) nonwoven fabrics should guarantee the stability of the network formation process for all selected batches of PP/PCL/CNT. Preliminary investigations indicate that to develop the required melt-blown process, the following technological parameters should be used:

- Extrusion zones temperature: 170°C/190°C/200°C/220°C/240°C/240°C/260°C,
- air temperature: 270°C,
- air velocity: 30–35 m^3/h,
- screw speed: 25–40 rpm, and
- die-collector distance: 25 cm.

The detailed processing conditions used for the manufacturing of a variant of the melt-blown nonwoven fabrics and their characteristics are presented in Tables IV and V. SEM micrographs of the samples are shown in Figure 3.

The application of technological parameters presented in Table IV guaranteed the stable formation of melt-blown nonwoven fabrics. In this article, only the samples collected during the stable technological process were subjected to further investigation. The results presented in Table IV show that the lowest values of

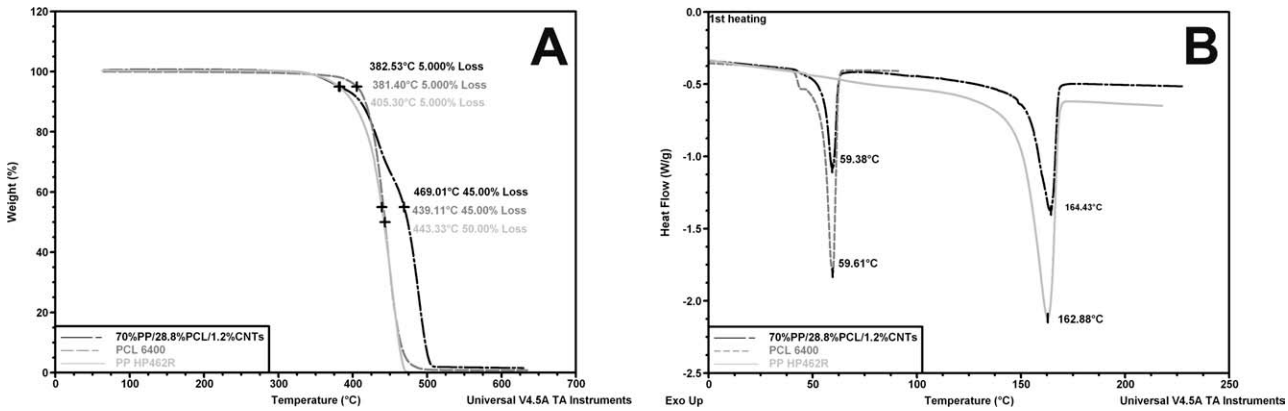

Figure 2. The TGA (A) and DSC (B) results from the raw materials studied.

Table IV. Processing Conditions and Electrical Characteristics of CPC Nonwoven Fabrics

Variants of melt-blown CPC nonwoven fabrics	Air velocity (m^3/h)	Screw speed (rpm)	Speed of the collector (rpm)	Surface resistance (Ω)	Vertical resistance (Ω)
50%PP/48%PCL/2%MWCNTs V2	30	25	0.1	3.9×10^{4a}	3.3×10^{4a}
50%PP/48%PCL/2%MWCNTs V4	30	35	0.1	3.1×10^{4a}	2.5×10^{4a}
60%PP/38.4%PCL/1.6%MWCNTs V1	30	25	0.1	9.3×10^{5b}	2.9×10^{5b}
60%PP/38.4%PCL/1.6%MWCNTs V3	30	35	0.1	1.5×10^{5b}	5.5×10^{4a}
70%PP/28.8%PCL/1.2%MWCNTs V1	30	25	0.1	8.0×10^{5b}	1.1×10^{5b}
70%PP/28.8%PCL/1.2%MWCNTs VV2	30	35	0.1	9.7×10^{5b}	3.1×10^{5b}
70%PP/28.8%PCL/1.2%MWCNTs V3	30	40	0.4	8.6×10^{5b}	2.5×10^{5b}
70%PP/28.8%PCL/1.2%MWCNTs V4	30	40	0.1	2.4×10^{5b}	1.3×10^{5b}

[a]Electrical resistance precision: $\pm 1 \times 10^2$ Ω, [b]Electrical resistance precision: $\pm 1 \times 10^3$ Ω.

Table V. Properties of CPC Nonwoven Fabrics

Variants of melt-blown CPC nonwoven fabrics	Mass per unit area (g/m^2)[a]	Thickness (mm)[b]	Apparent density (kg/m^3)[c]	Fiber dimension (μm)[d]	Crystallinity degree (%)
50%PP/48%PCL/2%MWCNTs V2	1016.25	3.46	293.70	2.07	52.4
50%PP/48%PCL/2%MWCNTs V4	1278.75	4.32	296.00	3.55	54.3
60%PP/38.4%PCL/1.6%MWCNTs V1	1305.00	4.24	307.78	2.92	58.0
60%PP/38.4%PCL/1.6%CNTs V3	1042.50	3.63	287.19	3.32	55.3
70%PP/28.8%PCL/1.2%MWCNTs V1	990.00	3.16	313.29	3.53	57.8
70%PP/28.8%PCL/1.2%MWCNTsV2	1326.25	4.19	316.52	3.95	55.8
70%PP/28.8%PCL/1.2%MWCNTs V3	460.00	1.74	264.37	2.78	56.5
70%PP/28.8%PCL/1.2%MWCNTs V4	1253.75	4.10	305.79	3.60	57.6

[a]Surface mass precision: ± 0.01 g/m^2, [b]Thickness precision: ± 0.01 mm, [c]Density precision: ± 0.01 kg/m^3, [d]Fiber dimension precision: ± 0.01 μm.

surface and vertical electrical resistance, on a level of 10^4 Ω, were achieved for samples containing 2% CNTs. The further decrease in content of this kind of nanoparticle in the polymer results in increased average values of the electrical resistances of melt-blown nonwoven fabrics to the order of 10^5 Ω, independent of the process parameters. This finding means that the main factor influencing the electrical conductivity of the melt-blown nonwoven fabrics is the optimum content of CNTs, similar to the percolation threshold, which should be in the range of 1–3% for the CPC system. Between variants, the smaller differences in surface and vertical electrical resistances result from the nature of the fibrous structures. In the case of materials, such as nonwoven fabrics, the electrical resistance is not only a function of fiber volume but also depends on the number of contacts

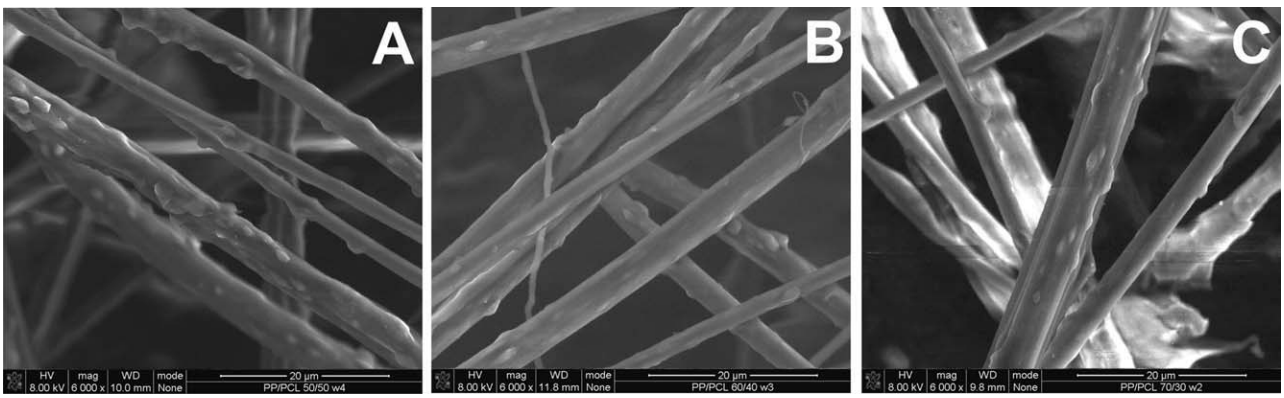

Figure 3. Visualization of macroscopic features and morphologies of nonwoven fabrics: (A) 50%PP/48%PCL/2%CNTs, (B) 60%PP/38.4%PCL/1.6%CNTs, and (C) 70%PP/28.8%PCL/1.2% CNTs.

Table VI. The Sensitivity of PP/PCL/CNT Nonwoven Fabrics to Heat Flux

Variants of melt-blown CPC nonwoven fabrics	First cycle		Second cycle		Third cycle		Fourth cycle	
	Temp[a] (°C)	R_{rel}[b] (%)	Temp[a] (°C)	R_{rel}[b] (%)	Temp[a] (°C)	R_{rel}[b] (%)	Temp[a] (°C)	R_{rel}[b] (%)
50%PP/48%PCL/2%MWCNTs V2	NTE		61.2	9.72	62.1	9.70	62	8.01
50%PP/48%PCL/2%MWCNTs V4	72.6	4.44	72.4	5.88	73.4	5.94	73.2	5.00
60%PP/38.4%PCL/1.6%MWCNTs V1	61.8	5.36	70.6	7.50	63.9	3.66	70.50	5.22
60%PP/38.4%PCL/1.6%MWCNTs V3	61.5	6.03	65.9	6.16	63.0	6.55	69.4	7.34
70%PP/28.8%PCL/1.2%MWCNTs V1	67.1	12.22	69.8	19.19	67.8	15.84	68.7	13.86
70%PP/28.8%PCL/1.2%MWCNTs V2	53.7	6.70	59.4	15.03	59.4	15.89	57.4	15.00
70%PP/28.8%PCL/1.2%MWCNTs V4	61.7	1.00	71.5	8.43	71.4	7.41	72.4	5.59
70%PP/28.8%PCL/1.2%MWCNTs V3	62.6	32.33	59.2	38.69	58.8	33.12	57.5	32.17

[a]Temperature at maximum value of resistance in the considered heating–cooling cycle, [b]Temperature precision: ±0.1°C.

between the fibers inside the discrete structures. The number of contacts is mainly a function of apparent density of nonwoven fabrics, fiber orientation, fiber diameter, etc. This aspect of the discussed phenomena was not a subject of our research. In Table V, the structural and morphological parameters of the nonwoven fabrics are presented. Regardless of technological parameters, all variants of obtained nonwoven fabrics were characterized by a higher crystallinity than the initial polymer. This result indicates slight orienting of the polymer structure during the melt-blown forming process of nonwoven fabrics. The applied process parameters guaranteed the stable formation of melt-blown nonwoven fabrics characterized by apparent density on a level of 264.37–313.52 kg/m^3 and fiber diameter on the level of 2.07–3.95 μm. Higher diameters were obtained by increasing the rotation speed of the extruder screw.

Thermal Sensitivity of Nonwoven CPC Fabrics

The sensitivity of the investigated samples of CPC nonwoven fabrics to heat flux was calculated according to Eq. (1) and is collected in Table VI.

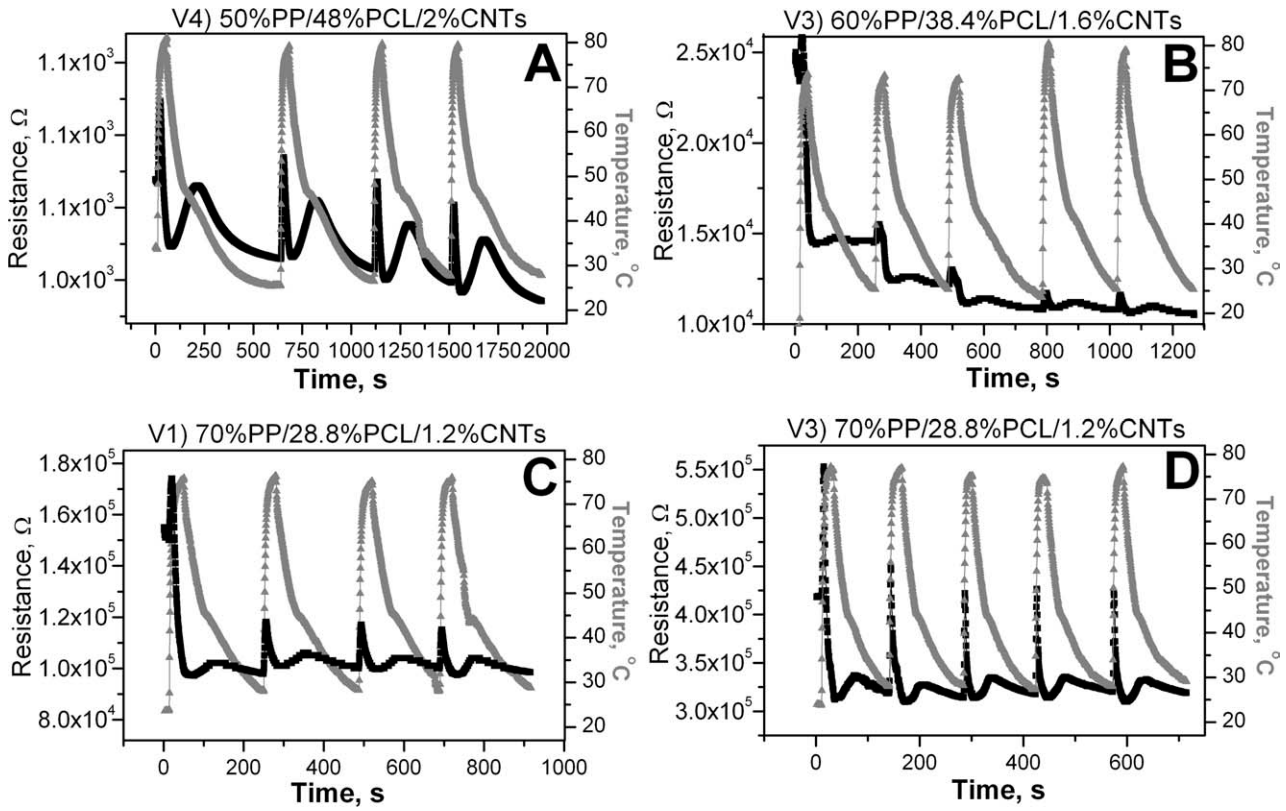

Figure 4. Change of resistance under the influence of temperature. (A) 50%PP/48%PCL/2%CNTs, (B) 60%PP/38.4%PCL/1.6%CNTs, and (C and D) 70%PP/28.8%PCL/1.2%CNTs.

Applied Polymer SCIENCE

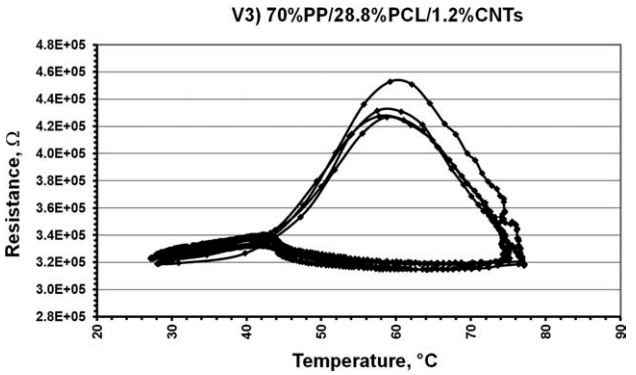

Figure 5. Change of resistance as a function of temperature for sample 70%PP/28.8%PCL/1.2%MWCNTs.

The samples were cut into rectangular shapes of dimensions 2 cm × 3 cm for investigation of sensor properties.

The investigation was repeated five times for each of the samples. In Table VI, the mean value of the results is being presented.

The results presented in Table IV and illustrated in Figure 3 indicate that the sensing properties of PP/PCL/MWCNTs nonwoven fabrics are strongly dependent on the following technological parameters of the melt-blown process: air velocity, screw speed, and the rate of rotation of collector; however, the most important role is played by the composition of the polymer batches. The nonwoven fabrics that best fulfilled the main assumption of the conducted research were composed of 30% PCL with MWCNTs Nanocyl®7000 dispersed in 70% of PP. For such a polymer composition, the positive temperature effect was clearly expressed. As the melting temperature of PCL was equal to 59.38°C for the first heating and 57.10°C for the second heating, a sharp increase in the electrical resistance of the melt-blown nonwoven fabric on the order of 15–38% was observed. The rate of increase in the electrical resistance for the discussed samples was also dependent on the other technological parameters. The most pronounced increase in electrical resistivity, resulting from disruption of the percolation path because of a phase change in PCL, was obtained at a screw speed of 40 rpm, air velocity of 30 m^3/h, and rate of rotation of the collecting drum equal to 0.4 rpm. Good results were also obtained for the same batch composition but at a screw speed of 35 rpm, air velocity of 30 m^3/h, and rate of rotation of the collector equal to 0.1 rpm. For both variants of samples, the maximum increase in the electrical resistance occurs in the PCL range of melting temperatures as determined using DSC for the polymer composition 70%PP/28.8%PCL/1.2%MWCNTs.

A further increase in temperature above the melting point of PCL, up to 80°C, resulted in a decrease in electrical resistance; indeed, even a negative temperature effect (NTE) is observed, i.e., electrical resistance assumes lower values than the initial resistance values determined at room temperature before subjecting the samples to thermal cycling. The NTE is the most

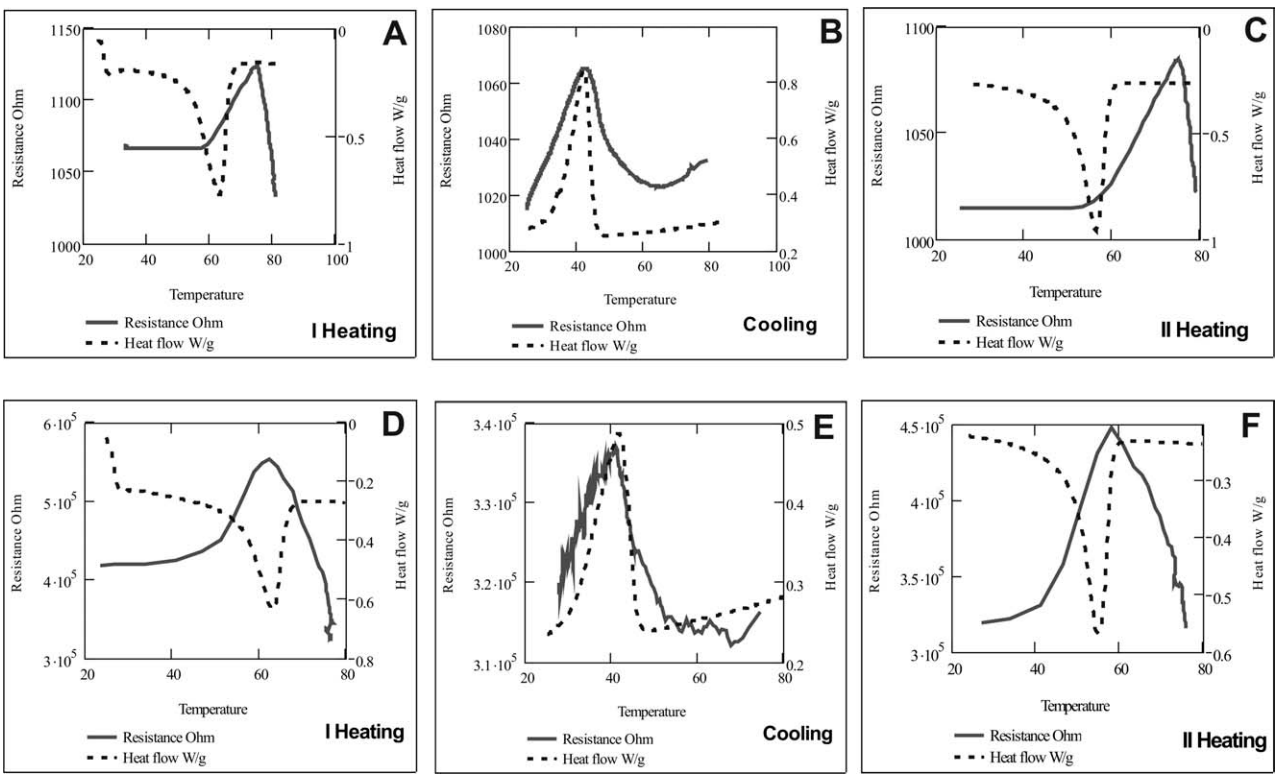

Figure 6. DSC and resistance curves for: (A) 50%PP/48%PCL/2%CNTs first heating, (B) 50%PP/48%PCL/2%CNTs cooling, (C) 50%PP/48%PCL/2%CNTs second heating, (D) 70%PP/28.8%PCL/1.2%CNTs first heating, (E) 70%PP/28.8%PCL/1.2%CNTs cooling, and (F) 70%PP/28.8%PCL/1.2%CNTs second heating.

pronounced for the first thermal cycle. For the optimal variants composed of 70%PP/28.8%PCL/1.2%MWCNTs, the resistance at the end of each heating–cooling cycle, except for the first cycle, is on the same order as that at the end of the first cycle, as shown in Figure 4(c,d). For the other polymer compositions, it was not possible to adjust the processing conditions to generate reproducible results. The drop in electrical resistance at the end of each cycle is greater than at the beginning. This phenomenon is illustrated in Figure 4(a,b). Moreover, the positive temperature effect is not well pronounced at the melting temperature of PCL determined by DSC for a composition of 50%PP/48%PCL/2%MWCNTs and 60%PP/38.4%PCL/1.6%MWCNTs. For some samples, the increase in electrical resistance under the heat flux appears even at a temperature of 70°C, i.e., 10°C greater than the melting temperature of PCL. This fact may result from the CNT content in the polymer and the development of percolation paths sensitive to the thermal expansion of PCL under the influence of the heat flux. It should be noted that the CNT content changes from a value of 2–1.2%. A higher CNT content may result in better-developed percolation paths that are more resistant to deformation.

The analysis of the changes in the electrical resistance also reveals the process of recrystallization of PCL. This process takes the maximum intensity at a temperature from the range 45.68–48.17°C. For all samples analyzed in this range of temperatures, a slight decrease in the electrical resistance was observed. The most pronounced of which belonged to the variant characterized by the highest content of PCL, i.e., for the 60%PP/38.4%PCL/1.6%MWCNTs variant, as shown in Figure 4(b).

Figure 5 shows the hysteresis for process heating and cooling of the sample 70%PP/28.8%PCL/1.2%MWCNTs, where the decrease in the electrical resistance was insignificant.

The relationships of the changes in electrical resistance to the changes in the microstructure of the polymer blends under the influence of temperature are illustrated in Figure 6. The comparison of the thermal sensory reaction of nonwoven fabrics with the DSC data obtained for the granulate clearly shows a correlation between the melt temperature of PCL and changes of resistance of the PP/PCL/MWCNTs composites. The results presented in Figure 6 confirm the periodic changes observed during the sensory studies (Figure 4). In our opinion, the interpretation of the thermal sensory of PP/PCL/MWCNTs composites as thermal structural changes of PCL is the most likely.

CONCLUSIONS

The conducted research confirms the application of conductive immiscible polymer blends as sensor materials for the manufacture of temperature-sensitive melt-blown nonwoven fabrics. It was demonstrated that the mechanism of temperature sensing in nanocomposite melt-blown nonwoven fabrics results from a PTC of resistivity effect when the temperature of the materials is increased to values near 60°C; a phase change in PCL and a conductor-to-insulation transition can be observed during this process. Reproducible results were obtained for the changes in the electrical resistance of melt-blown nonwoven fabrics composed of 70%PP/28.8%PCL/1.2%MWCNTs under four heating–cooling cycles. Additionally, it was observed that the optimal processing conditions for the manufacture of melt-blown nonwoven fabrics using the polymer batch composition specified above are as follows: a screw speed of 40 rpm, an air velocity of 30 m^3/h, and a rate of rotation of the collecting drum equal to 0.4 rpm.

ACKNOWLEDGMENTS

The authors gratefully acknowledge financial support from European Commission for the project entitled "Intelligent multi-reactive textiles integrating nano-filler based CPC-fibres" NMP2-CT-2006-026626 realized within the Six Framework Program for Research and Technological Development. The presented research was partially supported by this project.

REFERENCES

1. Iijima, S. *Nature* **1991,** *354*, 56.
2. Iijima, S.; Ichihadhi, T. *Nature* **1993,** *363*, 603.
3. Thostenson, E. T.; Ren, Z.; Chou, T. W. *Compos. Sci. Technol.* **2001,** *61*, 1899.
4. Huczko, A. *Carbon Nanotubes;* editor BEL, Warsaw, **2004;** ISBN 83-88442-86-4.
5. Yakobson, B. I.; Avouris, P. *Appl. Phys. B* **2001,** *80*, 287.
6. Ajayan, P. M.; Stephan, O.; Colliex, C.; Trouth, D. *Science* **1994,** *265*, 2112.
7. Haggenmueller, R.; Gommans, H. H.; Rinzler, A. G.; Fischer, J. E.; Winey, K. I. *Chem. Phys. Lett.* **2000,** *330*, 219.
8. Vigolo, B.; Penicaud, A.; Coulon, C.; Sauder, C.; Pailler, R.; Journet, C.; Bernier, P.; Poulin, P. *Science* **2000,** *290*, 1331.
9. Vigolo, B.; Poulin, P.; Lucas, M.; Launos, P.; Bernier, P. *Appl. Phys. Lett.* **2002,** *81*, 1210.
10. Dalton, A. B.; Collins, S.; Munoz, E.; Razal, J. M.; Ebron, V. H.; Ferrais, J. P.; Coleman, J. N.; Kim, B. G.; Baughman, R. H. *Nature* **2003,** *423*, 703.
11. Barisci, J. N.; Tahhan, M.; Wallace, G. G.; Badaire, S.; Vaugien, T.; Maugey, M.; Poulin, P. *Adv. Funct. Mater.* **2004,** *14*, 133.
12. Kearns, J. C.; Shambaugh, R. L. *J. Appl. Polym. Sci.* **2002,** *86*, 2079.
13. Moore, E. M.; Ortiz, D. L.; Marla, V. T.; Shambaugh, R. L.; Grady, B. P. *J. Appl. Polym. Sci.* **2004,** *93*, 2926.
14. Miaudet, P.; Badaire, S.; Maugey, M.; Derre, A.; Pichot, V.; Launois, P.; Poulin, P.; Zakri, C. *Nano Lett.* **2005,** *5*, 2212.
15. Chang, T. E.; Jensen, L. R.; Kisliuk, A.; Pipes, R. B.; Pyrz, R.; Sokolov, A. P. *Polymer* **2005,** *46*, 439.
16. Gao, J.; Itkis, M. E.; Yu, A.; Bekyarova, E.; Zhao, B.; Haddon, R. C. *J. Am. Chem. Soc.* **2005,** *127*, 3847.
17. Ko, F.; Gogotsi, Y.; Ali, A.; Naguib, N.; Ye, H. H.; Yang, G. L.; Li, C.; Willis, P. *Adv. Mater.* **2003,** *15*, 1161.
18. Sen, R.; Zhao, B.; Perea, D.; Itkis, M. E.; Hu, H.; Love, J.; Bekyarova, E.; Haddon, R. C. *Nano Lett.* **2004,** *4*, 459.
19. Pham, G. T.; Park, Y.-B.; Liang, Z.; Zhang, C.; Wang, B. *Compos. B* **2008,** *39*, 209.
20. Dharap, P.; Li, Z.; Nagarajaiah, S. *Nanotechnology* **2004,** *15*, 379.

21. Lua, J.; Kumara, B.; Castro, M.; Feller, J. F. *Sens. Actuators B* **2009,** *140*, 451.
22. Castro, M.; Lu, J.; Bruzaud, S.; Kumar, B.; Feller, J. F. *Carbon* **2009,** *47*, 1930.
23. Bai, H.; Shi, G. *Sensors* **2007,** *7*, 267.
24. Bavastrello, V.; Stura, E.; Carrara, S.; Erokhin, V.; Nicolini, C. *Sens. Actuators B* **2004,** *98*, 247.
25. Kobashi, K.; Villmow, T.; Andres, T.; Häußler, L.; Pötschke, P. *Smart Mater. Struct.* **2009,** *18*:035008, 15.
26. Kobashi, K.; Villmow, T.; Andres, T.; Pötschke, P. *Sens. Actuators B* **2008,** *134*, 787.
27. Kauffman, D. R.; Star, A. *Angew. Chem.* **2008,** *47*, 6550.
28. Shevade, A. V.; Ryan, M. A.; Homer, M. L.; Manfreda, A. M.; Zhou, H.; Manatt, K. S. *Sens. Actuators B* **2003,** *93*, 84.
29. Pumera, M.; Sanchez, S.; Ichinose, I.; Tang, J. *Sens. Actuators B* **2007,** *123*, 1195.
30. Merkoci, A.; Pumera, M.; Llopis, X.; Perez, B.; delValle, M.; Alegret, S. *Trends Anal. Chem.* **2005,** *24*, 826.
31. Feller, J. F.; Grohens, Y. *Sens. Actuators B* **2004,** *97*, 231.
32. Cochrane, C.; Koncar, V.; Lewandowski, M.; Dufour, C. *Polym. Compos. Sens.* **2007,** *7*, 473.
33. Cochrane, C.; Lewandowski, M.; Koncar, V. *Sensors* **2010,** *10*, 8291.
34. Pötschke, P.; Andresa, T.; Villmowa, T.; Pegela, S.; Brüniga, H.; Kobashi, K.; Fischera, D.; Häussle, L. *Compos. Sci. Technol.* **2010,** *70*, 343.
35. Krucińska, I.; Surma, B.; Chrzanowski, M. *Res. J. Text. Apparel* **2010,** *14*, 89.
36. Krucińska, I.; Urbaniak-Domagała, W.; Skrzetuska, E. *J. Appl. Polym. Sci.* **2011,** *121*, 483.
37. Srivastava, S.; Tchoudakov, R.; Narkis, M. *Polym. Eng. Sci.* **2000,** *40*, 1522.
38. Carmona, F.; Mouney, C. *J. Mater. Sci.* **1992,** *27*, 1322.
39. Rabiej, M.; Rabiej, S. Analiza Rentgenowskich Krzywych Dyfrakcyjnych Polimerów za Pomocą Programu Komputerowego WAXSFIT; Wydawnictwo ATH: Bielsko-Biała, **2006.**